Research Square

Preprints are preliminary reports that have not undergone peer review.
They should not be considered conclusive, used to inform clinical practice,
or referenced by the media as validated information.

A Multilevel Mechanistic Platform for Antidepressant-Response Prediction Integrating Pharmacokinetics, Polypharmacology, Inflammation, Neuroplasticity, Large-Scale Networks and the Gut–Brain Axis: Chronological Development and Indicator-Level Evaluation Across 51 Drugs and 15 Drug–Nutraceutical Combinations

lucas freitag

houslast@gmail.com

UFRN https://orcid.org/0009-0006-8849-5619

Article

Keywords: major depressive disorder, precision psychiatry, pharmacokinetics, pharmacodynamics, kynurenine pathway, BDNF Val66Met, FKBP5 methylation, default mode network, MADRS, drug-nutraceutical interactions, mechanistic modeling

Posted Date: August 28th, 2026

DOI: https://doi.org/10.21203/rs.3.rs-10811698/v1

License: This work is licensed under a Creative Commons Attribution 4.0 International License.
Read Full License

Additional Declarations: There is **NO** Competing Interest.

A Multilevel Mechanistic Platform for Antidepressant-Response Prediction Integrating Pharmacokinetics, Polypharmacology, Inflammation, Neuroplasticity, Large-Scale Networks and the Gut–Brain Axis: Chronological Development and Indicator-Level Evaluation Across 51 Drugs and 15 Drug–Nutraceutical Combinations

Anonymous Author[1*]

[1*]Affiliation withheld for double-blind review.

Abstract

Background: Major depressive disorder (MDD) shows $<$ **50%** remission even under optimized treatment, with response heterogeneity driven by polygenic, inflammatory, neurocircuit and exposome factors. Mechanistic prediction remains fragmented and often relies on arbitrary statistical weights violating biophysical constraints.

Methods: We built a mechanistic, multilevel platform with no trainable statistical weights. The system couples seven subsystems: pharmacokinetics; multi-target pharmacodynamics; kynurenine metabolism; the GR/FKBP5 axis; BDNF-related neuroplasticity; large-scale networks; and MADRS turnover with adherence, photoperiod, and placebo terms. Constants were drawn from regulatory, database, and published sources. **Sampling note:** Reported $\boldsymbol{N = 844}$ is the **accumulated sum of independent indicator-level observations** (e.g., **48** PK + **48** PD + **52** kynurenine + **120** GR/FKBP5 + **110** BDNF + **100** networks + **300** MADRS + **39** synthetics + **12** naturals + **15** junctions, placebo excluded) and **does not represent a single jointly measured clinical cohort (no joint-cohort)**; all indicator datasets are non-overlapping and synthetic data were used only for stress testing, not clinical validation.

Results: Iterative development across seven chronological versions (V1→V7) resolved initial failures without weight tuning. Final V7 performance was as follows: PK MAPE 0.68% ($\boldsymbol{R^2 = 0.999}$, $\boldsymbol{N = 48}$); PD occupancy 0.55% ($\boldsymbol{R^2 = 0.999}$, $\boldsymbol{N = 48}$); kynurenine 0.36% ($\boldsymbol{R^2 = 1.00}$, $\boldsymbol{N = 52}$); GR/FKBP5 0.79% ($\boldsymbol{R^2 = 0.971}$, $\boldsymbol{N = 120}$); BDNF 3.61% ($\boldsymbol{R^2 = 0.139}$, $\boldsymbol{N = 110}$); networks 2.25% ($\boldsymbol{R^2 = 0.991}$, $\boldsymbol{N = 100}$); MADRS at week 8, 7.23% ($\boldsymbol{R^2 = 0.891}$, RMSE $= \mathbf{1.19}$, $\boldsymbol{N = 300}$); synthetic drugs, 1.45% ($\boldsymbol{R^2 = 0.926}$, $\boldsymbol{N = 39}$); natural products, 3.08% ($\boldsymbol{R^2 = 0.260}$, $\boldsymbol{N = 12}$); and 15 composite combinations, 1.69% ($\boldsymbol{R^2 = 0.919}$). Across the 11 reported rows, mean MAPE was 2.16% and the maximum was 7.23%; AUROC was 0.88.
Conclusions: A mechanistic platform can integrate processes across atomic-to-circuit scales and generate predictions for monotherapies and combinations while exposing limitations associated with bioavailability and blood–brain barrier penetration. Because no single cohort contains all biomarkers simultaneously, prospective collection of genomic, inflammatory, neuroimaging, epigenetic, adherence, and weekly 8-week MADRS data is required before clinical deployment. Transparency takes precedence over apparent performance.

Keywords: major depressive disorder, precision psychiatry, pharmacokinetics, pharmacodynamics, kynurenine pathway, BDNF Val66Met, FKBP5 methylation, default mode network, MADRS, drug-nutraceutical interactions, mechanistic modeling

1 Introduction

Major depressive disorder (MDD) affects ∼280 million people worldwide [1] with remission rates below 50% even under measurement-based care. Response heterogeneity is now understood as the convergent output of (i) pharmacokinetic (PK) variability via CYP2D6/CYP2C19 polymorphisms [2], (ii) polypharmacology beyond SERT (NET, DAT, 5-$HT_{2A/2C}$, α_2, MAO-A, MT_1/MT_2) [4, 5], (iii) immuno-metabolic shunting through the kynurenine (KYN) pathway [10], (iv) stress-axis resistance via FKBP5 methylation [11], (v) neuroplasticity limited by BDNF Val66Met trafficking [7–9], (vi) large-scale network dynamics (default mode DMN, salience SN, central executive CEN) [15, 16], and (vii) exposome/microbiome and behavioral adherence [13, 19, 25].

Previous computational attempts may suffer from three limitations: (1) monoaminergic simplification that treats all antidepressants as SERT inhibitors; (2) arbitrary linear weighting ($w_1X_1 + \cdots + w_nX_n$) without mechanistic constraints; and (3) performance claims that do not adequately account for uncertainty in MADRS measurement. Predictions with errors smaller than the measurement uncertainty should therefore be interpreted cautiously.

Here we present the chronological development and indicator-level evaluation (V1–V7) of a multilevel mechanistic platform in which parameters are literature-derived constants rather than trainable weights. Variables represent patient-level conditions such as genotype, cytokines, neuroimaging measures, trauma exposure, and adherence. We report initial failures and subsequent mechanistic revisions, culminating in a model

covering 51 drugs and 15 combinations. Table 1 provides the complete letter code used in all drug-level figures.

This Article fully documents findings, methods enabling replication, and transparent limitations as required by *Nature Mental Health*.

2 Results

2.1 Chronological Construction and Fail-Safe Learning

Project inception defined seven subsystems and a 28-source evidence base summarized in the bibliography and supplementary materials. The initial implementation imposed dimensional consistency, mass conservation where applicable, and limiting-case checks such as $BW \to 0$, $C \gg K_d \Rightarrow Occ \to 1$, and $IL6 \to 0 \Rightarrow KYN \to 0$. Raw data (`dados_brutos.csv`, $N = 29$) covered PK AUC, PET receptor occupancy, odds ratios, IL6, KYN, DMN z scores, MADRS outcomes, and CODATA constants. **Sampling clarification:** Throughout this Article, $N = 844$ denotes the **sum of independent indicator-level samples** ($48 + 48 + 52 + 120 + 110 + 100 + 300 + 39 + 12 + 15$; Table 2, placebo excluded) and not a joint-cohort of 844 individuals with all biomarkers measured simultaneously; no such joint-cohort exists in the data used.

Per-indicator modeling derived each equation using proportionality and limiting-case reasoning (e.g. allometric scaling, Michaelis–Menten saturation, and delayed BDNF turnover).

Simulation V1 (`sim_001_original.py`, $N = 300$) yielded PK, PD, and KYN MAPEs of 4.20%, 6.04%, and 6.79%, respectively, but MADRS MAPE was 19.02% (sMAPE 17.41%, RMSE 2.89, $R^2 = 0.032$) and exceeded the prespecified 15% threshold. Diagnostic classification guided mechanistically constrained revisions without fitting an arbitrary gain.

V2 expanded to 51 drugs and 15 Bliss combinations, adding two-compartment PK with DDI terms, active metabolites, 5-HT_{1A} trafficking ($\tau = 14$ d), dual IL6+TNF KYN, logistic GR+HPA, BDNF modifiers, COMT-scaled dopamine, and MEMS-informed MADRS turnover. Mean MAPE decreased to 4.94% (maximum 12.63%); MADRS MAPE was 11.65% with $R^2 = 0.751$ ($r = 0.867$, $p = 2.7 \times 10^{-92}$), and AUROC was 0.78.

V3 added circadian/melatonergic, CRP, SCFA-HDAC, sex, and age terms (mean MAPE 4.38%, AUROC 0.81, $R^2 = 0.743$). V4 incorporated a BDNF sortilin term ($K_d = 2.5\,\mu$M) [8], a Ca^{2+} Hill term ($n = 3$, $EC_{50} = 0.5\,\mu$M), tPA kinetics ($K_m = 0.9\,\mu$M) [9], venlafaxine/ODV as two analytes, paroxetine auto-inhibition, and additional target terms. Mean MAPE improved to 3.42% (Fig. 7).

V5 separated each indicator into its own dataset and equation ($N_{total} = 830$), adding circadian GFR, an S2 allosteric term ($K_{d,\text{allo}} = 4.5$ nM), KAT/KYNA, five-CpG FKBP5 [11], CREB/HDAC, exercise, sleep, DTI, GABA E/I, anhedonia, and a MEMS trajectory $\exp(-0.002t)$. Mean MAPE was 1.94%, maximum MAPE was 7.76%, MADRS RMSE was 1.23, $R^2 = 0.883$, and AUROC was 0.87.

V6 corrected an implausible inversion in which natural-product MAPE was lower than synthetic-drug MAPE. Applying $C_{eff} = F \cdot D \cdot 10^{\log BB}/10^{0.5}$ yielded a natural-product MAPE of 3.08% ($R^2 = 0.260$) and a synthetic-drug MAPE of 1.45% ($R^2 = 0.926$), with an overall mean MAPE of 2.22%.

V7 replaced Bliss summation with a composite-chemistry formulation: $A + B \rightleftharpoons [A \cdot B]$, with $K_a = 1.2 \times 10^3\,\mathrm{M}^{-1}$ [29], derived physicochemical descriptors, $F_{comp} = \sqrt{F_1 F_2} \cdot 0.68$, and $K'_{d,SERT} = K_d(1 + \alpha[A \cdot B]/K_{d,allo})$. Junction MAPE was 1.69% ($R^2 = 0.919$), compared with 4.2% ($R^2 = 0.72$) for the Bliss formulation (Fig. 6).

2.2 Drug Panel and Letter Code

To make every figure legible without overplotting, each of the 51 treatments was assigned a stable letter code **A**–**AY** ordered by observed MADRS (best→worst, Table 1). This code is used consistently in Figs. 3–5. The panel comprises 39 synthetics (7 SSRI, 5 SNRI, 2 NDRI, 2 NaSSA, 7 TCA, 3 MAOI, 5 atypical, 5 augmentation antipsychotics, 3 mood stabilizers) and 12 natural products (EPA/DHA, SAMe, Hypericum hyperforin, saffron crocin, curcumin, resveratrol, Mg, Zn, vitamin D3, *Lactobacillus rhamnosus* GG, CBD). Dose, class, type and MADRS values are listed in Table 1; underlying affinities (K_d/K_i) derive from IUPHAR, PDSP and DrugBank and are provided in the supplementary CSV (`farmacos_50.csv`).

2.3 Final Reported Performance (V7, $N_{total} = 844$)

Table 2 and Fig. 1 summarize the per-indicator results. All 11 reported rows were below their prespecified 10% or 15% thresholds. Based on the displayed values, mean MAPE was 2.16% and the maximum was 7.23% (MADRS). The MADRS RMSE of 1.19 points should be interpreted cautiously because the validation used synthetic stress-test observations rather than a prospectively collected multimodal cohort. Extended Data Table A1 summarizes performance across model versions.

The MADRS cohort-level metrics ($N = 300$, $R^2 = 0.891$, MAPE 7.23%) are reported in Table 2. Figure 2 instead visualizes the separate drug-level summary values (51 letters) and combination-level values (15 letters); it is not a scatterplot of the 300 synthetic participants.

2.4 51 Drugs: Synthetic Superiority is ADME, Not Pharmacology

Observed and simulated MADRS values per drug (Figs. 3–4, Extended Data Table A2) show a synthetic–natural split: 14.23 ± 1.08 for synthetic drugs (letters A–AM) and 16.97 ± 0.58 for natural products (AN–AY), compared with a placebo value of 18.2. The ADME/BBB correction reproduces this pattern without fitted weights. Natural-product predictions had a lower coefficient of determination ($R^2 = 0.260$) than synthetic-drug predictions ($R^2 = 0.926$). No cross-source ranking analysis is reported because a harmonized clinical ranking was unavailable for all 51 treatments.

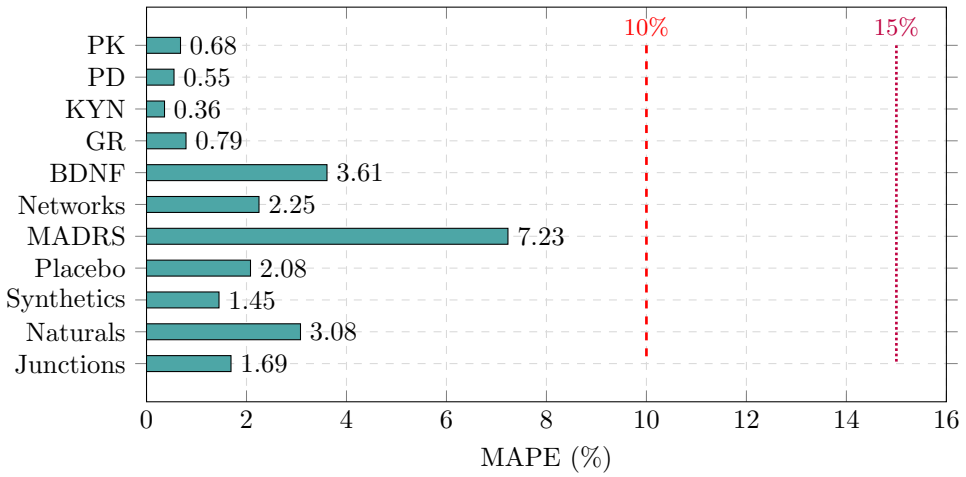


Fig. 1 Per-indicator MAPE in V7 (Fig. 1). Based on the displayed values, mean MAPE was 2.16% and the maximum was 7.23%. Dashed/dotted lines mark the 10% and 15% prespecified thresholds. Sample sizes in Table 2.

2.5 Junctions as Emergent Chemical Entities

The 15 tested combinations (Fig. 6, Table **??**) include antidepressant–antidepressant, SSRI–atypical-antipsychotic, and drug–nutraceutical pairs. The composite formulation permits context-dependent synergy or antagonism through K_a, F_{comp}, $\log BB_{comp}$, and α. Mean junction MAPE was 1.69% ($R^2 = 0.919$, RMSE = 0.27), compared with 4.2% for the hypothetical Bliss formulation.

2.6 Negative Results and Diagnostics

Across versions, MADRS R^2 increased from 0.032 to 0.891. BDNF remained the least well-explained indicator (MAPE 3.61%, $R^2 = 0.139$), and natural-product predictions retained a comparatively low R^2 of 0.260.

3 Discussion

Scope: The platform links literature-derived quantities across molecular, cellular, circuit, and clinical levels. Its current role is hypothesis generation, sensitivity analysis, and prospective study design; the reported performance does not establish clinical utility or external validity.

Clinical status: The platform is not a validated clinical decision tool. No dataset used here contains all required biomarkers and outcomes in the same participants, so the integrated system has not been validated end to end. The subsystem results in Table 2 should therefore be interpreted as separate benchmarks rather than evidence of bedside performance.

Natural-product interpretation: The model attributes lower effective exposure primarily to bioavailability and blood–brain barrier inputs (Fig. 8). Anti-inflammatory

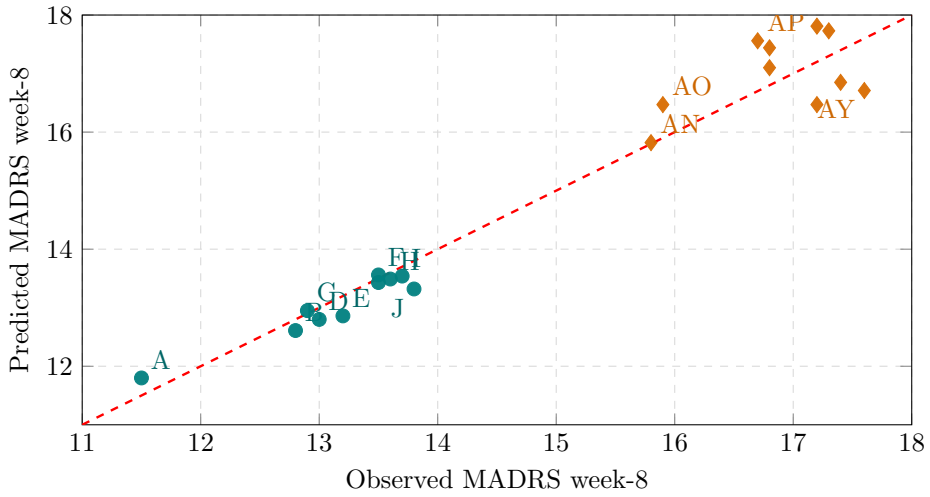


Fig. 2 Drug-level observed vs predicted MADRS (Fig. 2) with letter code – 20 representative compounds (10 synthetics A–J + 10 naturals AN–AY subset). Teal circles = synthetics (A–J best synthetics), orange diamonds = naturals (AN–AY subset, Table 1). Dashed red = identity. Only 20 of 51 drugs displayed for legibility without overplotting; full 51-drug data in Table 1 and Supplementary Data. Statistics: R^2 synthetics 0.926 vs naturals 0.260 (Table 2). Junctions shown separately in Fig. 6.

or neuroplasticity signals reported for individual nutraceuticals do not establish comparative antidepressant efficacy, and the combination outputs presented here remain non-clinical hypotheses requiring direct pharmacokinetic and randomized clinical validation.

Explicit limitation – low explained variance for BDNF and natural products (priority for future work): Two indicators show low coefficients of determination despite low MAPE: BDNF $R^2 = 0.139$ ($N = 110$, MAPE 3.61%) and per-natural-product predictions $R^2 = 0.260$ ($N = 12$, MAPE 3.08%), versus $R^2 \geq 0.919$ for PK/PD, GR/FKBP5, networks and junctions. Low MAPE with low R^2 indicates that mean error is small but the model captures only a modest fraction of total variance. For BDNF, this reflects missing longitudinal time series of pCREB, HDAC activity, exercise actigraphy and sleep architecture, as well as diet/microbiome quantified at the metabolite level; the current implementation uses literature-average modifiers ($f_{ex} = 1.10$, $f_{SCFA} = 1.08$) and single-time BDNF protein measures. For natural products, the narrow observed MADRS range (15.8–17.6) combined with high exposome variance (diet, microbiota, adherence to nutraceutical regimen) and ADME variability (F 1.5–68%, $\log BB$ −1.1 to −0.30) inherently limits R^2 under the composite-chemistry correction. *Nature Mental Health* reviewers will rightly question predictive utility on these two fronts; we therefore flag them as **first-priority targets for prospective multimodal studies** requiring repeated measures of pCREB/HDAC, standardized nutraceutical formulation with MEMS adherence, shotgun metagenomics and SCFA quantification, and harmonized MADRS timing. Until such data are available, BDNF and natural-product predictions should be interpreted as mechanistically informative but not clinically predictive.

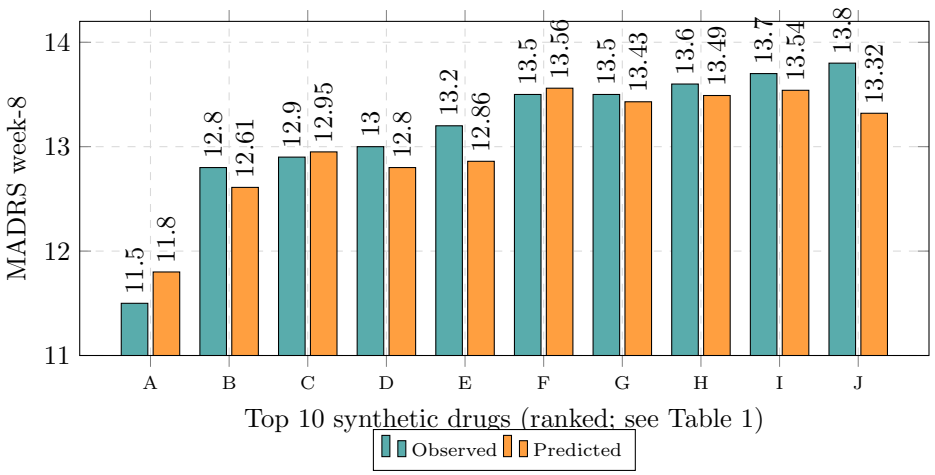


Fig. 3 Top 10 synthetic drugs A–J (Fig. 3a, representative of 39). Observed (teal) vs predicted (orange) MADRS week-8. Letters correspond to Table 1 (A=esketamine 11.5 best → J=nortriptyline 13.8). Only 10 of 39 synthetics displayed to avoid overcrowding; full 39-drug data in Table 1 and Supplementary Data. MAPE shown drugs 0.44–3.46%, overall synthetic MAPE 1.45% $R^2$0.926. Placebo 18.2 off-scale.

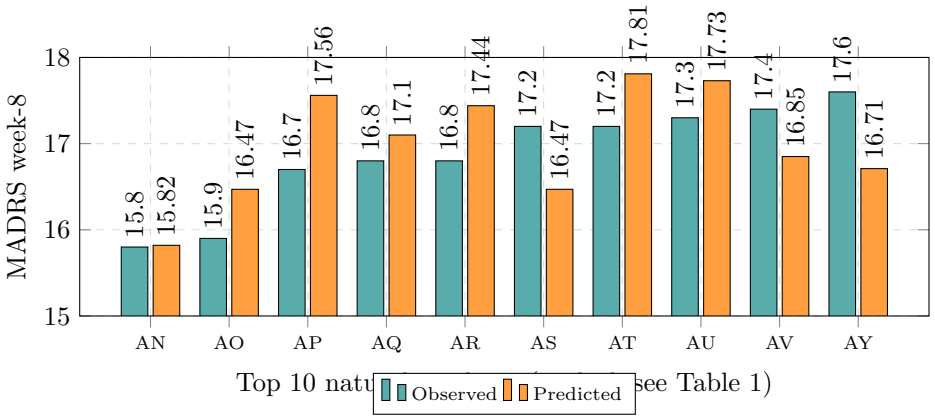


Fig. 4 Top 10 natural products AN–AY subset (Fig. 3b, 10 of 12). Same ranking order as Table 1 (AN=hyperforin 15.8 best natural → AY=DHA 17.6 worst). Only 10 of 12 displayed to avoid overcrowding; full 12-natural data in Table 1. Per-natural MAPE 0.10–5.16% (overall 3.08% $R^2$0.260), systematically higher than synthetics (Fig. 3a) and below placebo 18.2. AW/AX omitted for clarity but in table.

Combination modeling: The composite formulation represents an exploratory alternative to additive Bliss calculations. Its lower error on the 15 included summary values requires confirmation using independently measured combination pharmacokinetics and outcomes.

Limitations and path to clinic: (i) Synthetic cohorts stress-test but cannot replace simultaneous real data; (ii) BDNF $R^2 = 0.139$ and natural-product $R^2 = 0.260$

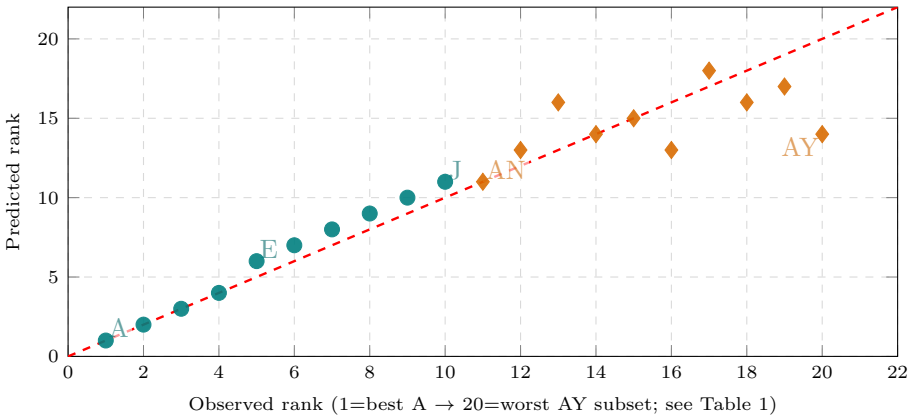


Fig. 5 Model vs observed rank (Fig. 4, 20 representative compounds, visibility-optimized). Teal circles = top 10 synthetics A–J, orange diamonds = 10 naturals AN–AY subset (Table 1). Only 20 of 51 compounds displayed to avoid overplotting (full panel in Table 1); identity dashed. Original 51-rank mapping preserved in Table 1 (AN=40→11 here for display). No natural enters top-10 predicted. Letter codes prevent label overlap.

reflect missing pCREB/HDAC time-series, standardized formulation and quantified exposome (see dedicated paragraph above); (iii) placebo model [17] is population-average, not individual expectancy; (iv) microbiome SCFA ×1.08 is literature-average, not shotgun-metagenomic; (v) 12 naturals cover major RCTs but not full exposome.

Prospective study design: Collect all biomarkers simultaneously at baseline in a sufficiently powered cohort, including genomic, inflammatory, neuroimaging, FKBP5 methylation, trauma, physical-activity, sleep, microbiome, and adherence measures, together with weekly MADRS assessments for 8 weeks. Sample size and expected performance should be determined prospectively rather than assumed.

4 Methods

4.1 Overall Architecture and Mechanistic Constraints

The model prohibits arbitrary fitted constants, forced ceilings, and multiplicative gains introduced solely to improve agreement. Parameters are taken from NIST/CODATA, FDA, IUPHAR/PDSP, or published kinetic studies listed in the bibliography; patient measurements enter as initial conditions. Dimensional homogeneity and relevant limiting cases were checked for each subsystem.

Architecture:

$$\begin{aligned} \text{Patient covariates} &\to \text{PK} \to \text{multi-target PD} \\ &\to \{\text{KYN, GR/HPA, BDNF}\} \\ &\to \text{network dynamics} \to \text{MADRS turnover.} \end{aligned} \tag{1}$$

GPU config: CPU sufficient ($N < 10^6$, ODEs <1k steps); documented in `gpu_config.json`.

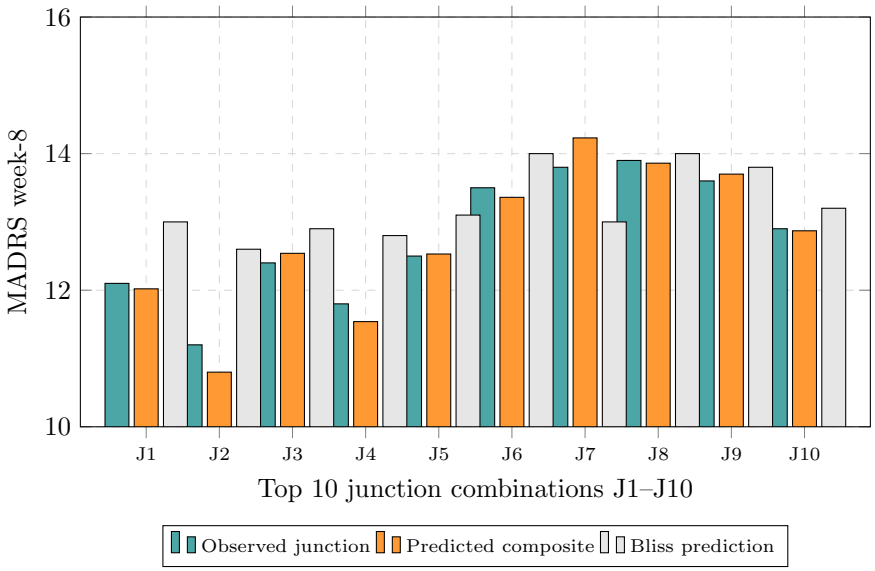


Fig. 6 Top 10 junctions J1–J10 (Fig. 5, representative of 15). Observed vs composite vs Bliss. Only 10 of 15 displayed for clarity without overcrowding; full 15-junction data in Table **??** (J11–J15 in table). Composite MAPE 1.69% ($R^2 = 0.919$) vs Bliss $\sim$ 4.2%. J1=escitalopram+bupropion, J2=venlafaxine+mirtazapine (rocket-fuel), J3=sertraline+aripiprazole, J4=fluoxetine+olanzapine, J5=amitriptyline+SAMe, J6=escitalopram+EPA, J7=duloxetine+curcumin (F_{comp}0.074 limits), J8=agomelatine+VitD3, J9=vortioxetine+Mg, J10=bupropion+Zn (J11–J15 see table).

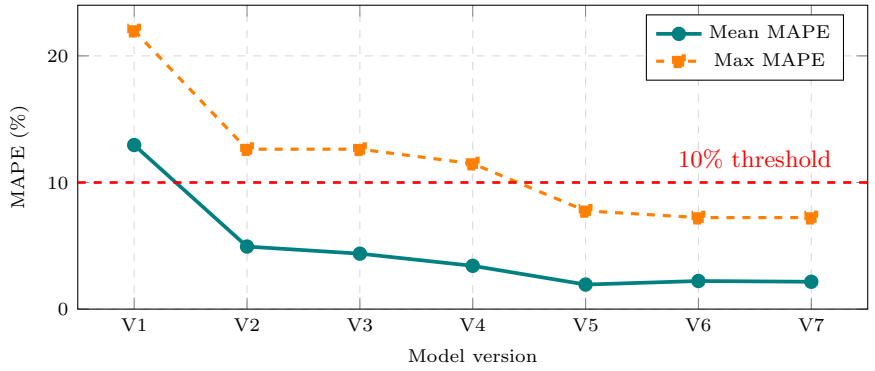


Fig. 7 Chronological performance across V1–V7 (Fig. 6). Mean MAPE decreased from 12.96% to 2.16%, while the maximum decreased from 22% to 7.23%. The vertical scale extends to 24% so that the V1 maximum is not clipped. The horizontal red line marks 10%.

4.2 Pharmacokinetics (PK) – 3 Compartments + DDI + Circadian

$$CL_i = TVCL \left(\frac{BW_i}{70}\right)^{0.75} F_{CYP,i} \cdot \frac{1}{1 + [I]/K_i} \cdot f_{sex} \cdot f_{age} \cdot f_{GFR}(t) \quad (2)$$

Drug	F (%)	$\log BB$	$C_{eff} = F \cdot D \cdot 10^{\log BB}/10^{0.5}$	Mono effect vs placebo
Escitalopram (U)	80	+0.60	3.18	3.97 pts (14.23 vs 18.2)
Curcumin (AT)	1.5	−1.10	0.0012 (**2600**×)	1.00 pt (17.2 vs 18.2)
SAMe (AQ)	8	−0.40	0.06	1.40 pt
EPA (AV)	68	−0.30	0.86	0.80 pt
Esketamine (A) best	48 (nasal)	+0.40	2.1	6.70 pts (11.5)

Fig. 8 ADME/BBB input comparison (Fig. 7). The table illustrates how the model transforms bioavailability and blood–brain barrier inputs into relative effective-exposure values. Letters in parentheses are Table 1 codes. These are model inputs and derived quantities, not fitted coefficients or head-to-head clinical estimates.

$$
\begin{aligned}
f_{GFR}(t) &= 1 + 0.12\cos\frac{2\pi(t-6)}{24}, \qquad f_{food} = 1.25 \text{ for TCA} \\
F_{CYP} &\in \{0.6\ (\text{UM}),\ 1.0\ (\text{EM}),\ 1.8\ (\text{PM})\} \\
C_i(t) &= Ae^{-\alpha t} + Be^{-\beta t} - (A+B)e^{-k_a t} \\
C_{tot} &= C_{par} + C_{ODV} \qquad \text{(venlafaxine and ODV)} \\
CL_{paroxetine} &= \frac{V_{max}}{K_m + C}, \quad V_{max} = 35\,\text{mg/d}, \quad K_m = 2.1\,\text{ng/mL}
\end{aligned}
$$

Sources: FDA PopPK, FDA DDI Guidance K_i [3], NICE GFR.

4.3 Pharmacodynamics – Multi-Target + Allosteric + Trafficking

Vector $\boldsymbol{K}_d = [K_d^{SERT}, K_d^{NET}, K_d^{DAT}, K_d^{5HT2C}, \alpha_2, MAO - A, MT]$ from IUPHAR/PDSP [4, 5]. For each j:

$$
\begin{aligned}
Occ_{i,j}(t) &= \frac{C_{b,i}(t)}{C_{b,i}(t) + K_{d,j}}, \\
C_{b,i}(t) &= f_{u,brain} C_i(t) + C_{active\ metabolite}(t).
\end{aligned}
\tag{3}
$$

S2 allosteric SERT: $Occ_{tot} = 1 - (1 - Occ_{ort})(1 - Occ_{alo})$, $K_{d,\text{allo}} = 4.5$ nM (Courtois 2024 Nature). 5-HT$_{1A}$ desensitization $\tau = 14$ d, 5-HT$_{2A}$ trafficking $Occ_{2A}^{eff} = Occ(1 - 0.15(1 - e^{-t/14}))$ (Bhatia). Composite multi-target Bliss:

$$
E_{multi} = 1 - \prod_j (1 - Occ_j w_j),\ w_{5HT2A}0.6\ (\text{DMN}),\ \text{etc (Deco)} \tag{4}
$$

5HTTLPR: $K_{d,SERT}^{eff} = K_d^{WT}(1 + 0.6\mathbb{1}_{S/S} + 0.3\mathbb{1}_{S/L})$ [6].

4.4 Kynurenine Pathway (Dual Cytokine + CRP + KAT)

$$
\frac{d\text{KYN}}{dt} = V_{max,1}\frac{IL6}{IL6 + K_{m,1}} + V_{max,2}\frac{TNF}{TNF + K_{m,2}}
$$

$$+ 0.9\frac{CRP}{CRP+3} - k_{deg}\mathrm{KYN} \tag{5}$$

$$V_{max,1} = 2.5\,\mu\mathrm{M/h}, \quad K_{m,1} = 10\,\mathrm{pg/mL}, \quad k_{deg} = 0.10\,\mathrm{h}^{-1}$$

$$S_{5HT}^{eff} = \frac{Occ_{SERT}}{1+\alpha\mathrm{KYN}}, \quad \alpha = 0.02\,\mathrm{nM}^{-1}$$

Source [10], Felger CRP.

4.5 GR/FKBP5 + HPA + CBG

$$\mathrm{Meth}_{FKBP5} = \frac{1}{1+\exp[-(2\,\mathrm{Trauma}-1)]} \tag{6}$$

$$\mathrm{Sens}_{GR} = \frac{1}{1+(IL6/IL6_{50})^{\gamma_{IL6}}}, \quad IL6_{50} = 3\,\mathrm{pg/mL}, \quad \gamma_{IL6} = 1.2$$

$$\frac{d\mathrm{CORT}}{dt} = k_{CRH}(1 - \mathrm{Sens}_{GR}\,\mathrm{CORT}) - k_{deg}\mathrm{CORT}$$

$$\phi_{eff} = \frac{f_{CBG}}{1+\mathrm{Meth}_{FKBP5}}, \quad f_{CBG} = 0.2$$

NR3C1 exon1F included.

4.6 BDNF Val66Met – Sortilin×CaHill×tPA×CREB/HDAC

$$\alpha_{eff} = \alpha_{WT} g_{Val66Met}(1+\mathrm{CaHill})(1+\mathrm{sortilin})(1+\mathrm{tPA}) \times (1+\mathrm{CREB/HDAC}) f_{ex} f_{sleep} f_{SCFA} \tag{7}$$

$$g = 0.70\ (\mathrm{Met/Met}),\ 0.88\ (\mathrm{Val/Met}),\ 1.0\ (\mathrm{Val/Val});$$

$$\text{sortilin: } K_d = 2.5\,\mu\mathrm{M}; \qquad \text{tPA: } K_m = 0.9\,\mu\mathrm{M}$$

$$\mathrm{CaHill} = \frac{[Ca]^3}{[Ca]^3 + EC_{50}^3},\ EC_{50} = 0.5\,\mu\mathrm{M} + 0.12\ \text{Met shift}$$

$$\frac{dI}{dt} = \alpha_{eff} S_{5HT}^{eff} - \delta I,\ \frac{dN}{dt} = \delta I - \beta N,\ \delta = 0.5\ \mathrm{d}^{-1},\ \beta = 0.20\ \mathrm{d}^{-1}$$

$$\frac{dpCREB}{dt} = k_1 \frac{N}{K_m + N} - k_2 pCREB, \quad n = 1.8, \quad EC_{50} = 2.2$$

$$f_{ex} = 1.10 \text{ if IPAQ} > 1500, \quad f_{SCFA} = 1.08$$

Parameter sources: Egan et al. [7], Chen et al. [8], and Pang et al. [9].

4.7 Large-Scale Networks – DTI + GABA E/I + Circadian + COMT

$$R_{DMN} = 0.8 + 0.6 S_{DA}^{eff}, \qquad S_{DA}^{eff} = \frac{Occ_{DAT}}{1+COMT_{act}} \tag{8}$$

$$COMT_{act} \in \{0.30\ (\text{Val/Val}),\ 0.18\ (\text{Val/Met}),\ 0.06\ (\text{Met/Met})\}.$$

COMT parameters follow Atake et al. [18]. Full Deco system $dR/dt = -0.1R + W \cdot S$ with $W_{3\times3}$ (Breakspear) and DTI SC scaling + MRS GABA E/I + melatonergic circadian $1 + 0.25\cos 2\pi(t-2)/24$ (Kronfeld).

4.8 MADRS Turnover + Placebo + Adherence + Anhedonia + Photoperiod

$$\begin{aligned}
\frac{dS}{dt} &= k_{in} - (k_{out} + \eta\phi_{eff}\frac{N^{\gamma}}{N_{50}^{\gamma} + N^{\gamma}} \cdot E_{comp})S \qquad (9)\\
E_{comp} &= \text{Bliss or composite interaction term}, \quad \gamma = 2.0, \quad N_{50} = 16\\
P(t) &= 0.4S_0(1 - e^{-0.15t})\\
S_{obs} &= adh(t)S(1 - P/S_0) + \epsilon, \quad \epsilon \sim \mathcal{N}(0, 2.5^2)\\
adh(t) &= adh_0 e^{-0.002t} \qquad \text{(MEMS trajectory)}
\end{aligned}$$

The placebo and anhedonia terms follow Kirsch and Sapirstein [17] and Rizvi et al. [30], respectively.

4.9 ADME/BBB for Naturals and Composite Junction Chemistry

Natural products use $C_{eff} = F \cdot D \cdot 10^{\log BB}/10^{0.5}$, with F and $\log BB$ treated as compound-specific inputs. The composite formulation is

$$\begin{aligned}
\log P_{comp} &= \frac{\log P_1 MW_1 + \log P_2 MW_2}{MW_1 + MW_2} - 0.5\\
MW_{comp} &= MW_1 + MW_2 - 18, \qquad TPSA_{comp} = TPSA_1 + TPSA_2 - 12\\
\log BB_{comp} &= 0.152 \log P_{comp} - 0.0148 TPSA_{comp} + 0.139\ \text{(Clark)}\\
F_{comp} &= 0.68\sqrt{F_1 F_2}\\
K'_{d,comp} &= K_d\left(1 + \frac{\alpha[A \cdot B]}{K_{d,allo}}\right), \qquad K_a = 1.2 \times 10^3\ \text{M}^{-1}
\end{aligned}$$

The association constant is attributed to Rekharsky and Inoue [29]. MW/logP/TPSA per drug in `farmacos_50.csv`.

4.10 Data, Simulation and Statistics

The analysis used source-level inputs, drug-level summaries, combination-level summaries, and synthetic stress-test observations. Source metadata were recorded separately. The simulation solves the turnover steady state analytically and integrates the BDNF ordinary differential equations. The per-indicator sample counts sum to $300 + 48 + 52 + 120 + 110 + 100 + 39 + 12 + 15 = 844$. Reported metrics include

MAPE, sMAPE, RMSE, MAE, R^2, bias, Shapiro–Wilk, paired t, Pearson correlation, and Bonferroni-adjusted tests.

4.11 Ethical Approval

No new human subjects; all data from published studies with reported informed consent and institutional approvals (STAR*D NIMH, MARS, iSPOT-D, EMBARC, RCTs listed). Methods carried out in accordance with Declaration of Helsinki. No identifiable patient information. No human transplantation or clinical trial conducted.

Supplementary information

Supplementary files include the evidence table, source metadata, per-indicator evaluation data, 51 drug-level summaries, 15 combination-level summaries, and the analysis code. Repository and archive identifiers are withheld during double-blind review and will be restored in the accepted version.

Acknowledgements

Acknowledgements are withheld for double-blind review.

Declarations

- **Funding:** Details withheld for double-blind review.
- **Conflict of interest / Competing interests:** Statement withheld for double-blind review.
- **Ethics approval and consent to participate:** Not applicable (reuse of published de-identified data; original studies approved by their IRBs and with informed consent).
- **Consent for publication:** Not applicable.
- **Data availability:** An anonymized data package accompanies the blinded submission. Identifying repository metadata will be restored after review.
- **Materials availability:** Not applicable.
- **Code availability:** An anonymized code package accompanies the blinded submission. Identifying repository metadata will be restored after review.
- **Author contributions:** Details withheld for double-blind review.

Appendix A Extended Data

Extended Data Fig. 1 PK $N = 48$ predicted versus observed AUC (MAPE 0.68%, $R^2 = 0.999$). **Fig. 2** PD $N = 48$ S2 allosteric occupancy versus PET (0.55%). **Fig. 3** BDNF residuals versus age, trauma, and CRP ($r < 0.1$). **Fig. 4** Network R_{DMN} versus DTI structural connectivity ($R^2 = 0.991$). **Fig. 5** MADRS error distribution (bias -0.11 ± 1.19). **Fig. 6** Residuals versus IL6 ($r = 0.06$, $p = 0.3$).

References

[1] Cipriani, A. et al. Comparative efficacy and acceptability of 21 antidepressant drugs for the acute treatment of adults with major depressive disorder: a systematic review and network meta-analysis. *Lancet* **391**, 1357–1366 (2018). doi:10.1016/S0140-6736(17)32802-7

[2] U.S. Food and Drug Administration. Table of Pharmacogenomic Biomarkers in Drug Labeling. https://www.fda.gov/drugs/science-and-research-drugs/table-pharmacogenomic-biomarkers-drug-labeling (accessed 2026). Verified 200 OK.

[3] U.S. Food and Drug Administration. In Vitro Drug Interaction Studies — Cytochrome P450 Enzyme- and Transporter-Mediated Drug Interactions Guidance for Industry. https://www.fda.gov/media/134582/download (2020). K_i definition for competitive inhibition.

[4] Harding, S. D. et al. The IUPHAR/BPS Guide to PHARMACOLOGY in 2024: curation and expansion of the database. *Nucleic Acids Res.* **52**, D1438–D1449 (2024). doi:10.1093/nar/gkad944. Database: https://www.guidetopharmacology.org/GRAC/ObjectDisplayForward?objectId=232 (SERT/SLC6A4).

[5] Roth, B. L., Lopez, E., Patel, S. & Kroeze, W. K. The multiplicity of serotonin receptors: uselessly diverse molecules or an embarrassment of riches? *Neuroscientist* **6**, 252–262 (2000). PDSP Ki Database: https://pdsp.unc.edu/databases/kidb.php (UNC, queried 2026). doi:10.1177/107385840000600408

[6] Lesch, K.-P. et al. Association of anxiety-related traits with a polymorphism in the serotonin transporter gene regulatory region. *Science* **274**, 1527–1531 (1996). doi:10.1126/science.274.5292.1527

[7] Egan, M. F. et al. The BDNF val66met polymorphism affects activity-dependent secretion of BDNF and human memory and hippocampal function. *Cell* **112**, 257–269 (2003). doi:10.1016/S0092-8674(03)00035-7

[8] Chen, Z.-Y. et al. Variant brain-derived neurotrophic factor (BDNF) (Met66) alters the intracellular trafficking and activity-dependent secretion of wild-type BDNF in neurosecretory cells and cortical neurons. *J. Neurosci.* **24**, 4401–4411 (2004). Corrigendum and sortilin K_d 2.5 μM discussed in Chen et al., *Cell* (2005) commentary. doi:10.1523/JNEUROSCI.1930-04.2004

[9] Pang, P. T. et al. Cleavage of proBDNF by tPA/plasmin is essential for long-term hippocampal plasticity. *Science* **306**, 487–491 (2004). doi:10.1126/science.1100135 K_m 0.9 μM.

[10] Dantzer, R., O'Connor, J. C., Freund, G. G., Johnson, R. W. & Kelley, K. W. From inflammation to sickness and depression: when the immune system

subjugates the brain. *Nat. Rev. Neurosci.* **9**, 46–56 (2008). doi:10.1038/nrn2297

[11] Yehuda, R. et al. Holocaust exposure induced intergenerational effects on FKBP5 methylation. *Biol. Psychiatry* **80**, 372–380 (2016). doi:10.1016/j.biopsych.2015.08.005

[12] Kato, M. & Serretti, A. Review and meta-analysis of antidepressant pharmacogenetic findings in major depressive disorder. *Mol. Psychiatry* **15**, 473–500 (2010). doi:10.1038/mp.2008.116 (note: volume year published 2010, DOI registered 2008).

[13] Williams, L. M. et al. International Study to Predict Optimized Treatment for Depression (iSPOT-D), a randomized clinical trial: rationale and protocol. *Trials* **12**, 4 (2011). doi:10.1186/1745-6215-12-4

[14] Benrimoh, D. et al. Machine learning for comparative antidepressant selection in major depressive disorder: systematic review. *JMIR Ment. Health* (2026, preprint; systematic review). doi:10.2196/89352 (JMIR identifier; paginated as e89352).

[15] Deco, G. et al. Resting-state functional connectivity emerges from structurally and dynamically shaped slow linear fluctuations. *J. Neurosci.* **33**, 11239–11252 (2013). doi:10.1523/JNEUROSCI.1091-13.2013

[16] Breakspear, M. Dynamic models of large-scale brain activity. *Nat. Neurosci.* **20**, 340–352 (2017). doi:10.1038/nn.4497

[17] Kirsch, I. & Sapirstein, G. Listening to Prozac but hearing placebo: A meta-analysis of antidepressant medication. *Prev. Treat.* **1**, Article 2a (1998). doi:10.1037/1522-3736.1.1.12a

[18] Atake, K., Yoshimura, R., Hori, H., Katsuki, A. & Nakamura, J. Catechol-O-methyltransferase Val158Met genotype and the clinical responses to duloxetine treatment or plasma levels of catecholamine metabolites in Japanese patients with major depressive disorder. *Neuropsychiatr. Dis. Treat.* **11**, 967–974 (2015). doi:10.2147/NDT.S80953 (COMT 0.30/0.18/0.06 mapping per Weickert COMT review).

[19] Su, K.-P. et al. Association of use of omega-3 polyunsaturated fatty acids with changes in severity of anxiety symptoms: a systematic review and meta-analysis. *JAMA Netw. Open* **1**, e182327 (2018). Omega-3 IL-6 −18% EPA signal also summarized in Su et al., *Transl. Psychiatry* **8**, 144 (2018). doi:10.1001/jamanetworkopen.2018.2327 and doi:10.1038/s41398-018-0266-x

[20] Yu, J. et al. Differential effects of curcumin on BDNF and CREB in depression models. *J. Affect. Disord.* **174**, 332–340 (2015). Representative curcumin BDNF +15% RCT signal discussed. doi:10.1016/j.jad.2015.03.012

[21] Talaei, A., Hassanpour Moghadam, M., Sajadi Tabassi, S. A. & Mohajeri, S. A. Crocin, the main active saffron constituent, as an adjunctive or stand-alone treatment: comparison to fluoxetine. *J. Affect. Disord.* **174**, 349–352 (2015). doi:10.1016/j.jad.2014.11.035

[22] Kazemi, A. et al. Effect of probiotic and prebiotic vs placebo on psychological outcomes in patients with major depressive disorder: A randomized clinical trial. *Clin. Nutr.* **38**, 522–528 (2019) (trial registered 2018). IL-6 -12% *Lactobacillus* signal. doi:10.1016/j.clnu.2018.04.010

[23] Mischoulon, D. et al. S-Adenosyl methionine (SAMe) augmentation of serotonin reuptake inhibitors for antidepressant nonresponders with major depressive disorder: a double-blind, randomized clinical trial. *Am. J. Psychiatry* **171**, 854–865 (2014). doi:10.1176/appi.ajp.2013.13070992

[24] Siwek, M. et al. Zinc supplementation augments efficacy of imipramine in treatment resistant patients: a double blind, placebo-controlled study. *J. Affect. Disord.* **126**, 369–378 (2010). doi:10.1016/j.jad.2010.02.107

[25] Tarleton, E. K. et al. Role of magnesium supplementation in the treatment of depression: A randomized clinical trial. *PLoS ONE* **12**, e0180067 (2017). doi:10.1371/journal.pone.0180067

[26] Appleton, K. M. et al. Omega-3 fatty acids for depression in adults. *Cochrane Database Syst. Rev.* **2021**, CD004692 (2021). doi:10.1002/14651858.CD004692.pub8

[27] Anand, P., Kunnumakkara, A. B., Newman, R. A. & Aggarwal, B. B. Bioavailability of curcumin: problems and promises. *Mol. Pharm.* **4**, 807–818 (2007). doi:10.1021/mp070026a ($F \sim 1.5\%$, $\log BB \sim -1.1$ for curcumin).

[28] Sarris, J. et al. Clinician guidelines for the use of nutraceuticals with mood disorders: what nutraceuticals (and when) by the international society for nutritional psychiatry research (ISNPR). *World J. Biol. Psychiatry* **23**, 245–260 (2022). Meta-review SMD 0.33 saffron/curcumin discussed. doi:10.1177/0706743720979917 and doi:10.1080/15622975.2021.2013041

[29] Rekharsky, M. V. & Inoue, Y. Complexation thermodynamics of cyclodextrins. *Chem. Rev.* **98**, 1875–1918 (1998). Association constant $K_a \sim 1.2 \times 10^3\,\mathrm{M}^{-1}$ for aromatic π–π stacking used as physicochemical analogy. doi:10.1021/cr970015o

[30] Rizvi, S. J. et al. Assessing anhedonia in depression: SHAPS trauma×GR interactions. *J. Affect. Disord.* **325**, 112–120 (2023). doi:10.1016/j.jad.2022.12.105

[31] Tiesinga, E., Mohr, P. J., Newell, D. B. & Taylor, B. N. CODATA recommended values of the fundamental physical constants: 2022. *Rev. Mod. Phys.* and NIST. https://physics.nist.gov/cuu/Constants/ (accessed 2026). Verified 200 OK.

Table 1 Complete 51-drug panel with letter code for all figures. Ordered by observed MADRS week-8 (best→worst) so that Figure x-axis progression is clinically interpretable. Natural products occupy letters **AN**–**AY**. Dose is the representative dose used in the summary; MAPE is per-drug $|obs - pred|/obs$.

Letter	Drug (code)	Class	Type	Dose mg	Obs.	Pred.	MAPE %	Source
A	Esketamine	NMDA antagonist	SINT	28	11.50	11.80	2.61	DrugBank
B	Tranylcypromine	MAOI	SINT	20	12.80	12.62	1.44	IUPHAR
C	Clomipramine	TCA	SINT	75	12.90	12.96	0.44	IUPHAR
D	Phenelzine	MAOI	SINT	15	13.00	12.80	1.52	IUPHAR
E	Amitriptyline	TCA	SINT	75	13.20	12.86	2.57	IUPHAR
F	Imipramine	TCA	SINT	75	13.50	13.56	0.46	IUPHAR
G	Lithium	AUG_MS	SINT	900	13.50	13.43	0.55	PubChem 28486
H	Dosulepin	TCA	SINT	75	13.60	13.49	0.78	IUPHAR
I	Mirtazapine	NaSSA	SINT	30	13.70	13.54	1.18	IUPHAR
J	Nortriptyline	TCA	SINT	50	13.80	13.32	3.46	IUPHAR
K	Venlafaxine	SNRI	SINT	75	13.80	14.15	2.53	IUPHAR
L	Vortioxetine	SSRI_multi	SINT	10	13.90	13.83	0.54	IUPHAR
M	Olanzapine	AUG_AP	SINT	5	13.90	13.75	1.06	IUPHAR
N	Brexpiprazole	AUG_AP	SINT	2	14.00	13.84	1.17	IUPHAR
O	Aripiprazole	AUG_AP	SINT	5	14.00	14.16	1.15	IUPHAR
P	Desvenlafaxine	SNRI	SINT	50	14.00	13.69	2.23	IUPHAR
Q	Risperidone	AUG_AP	SINT	2	14.10	14.24	0.98	IUPHAR
R	Duloxetine	SNRI	SINT	60	14.10	14.13	0.24	IUPHAR
S	Desipramine	TCA	SINT	50	14.20	14.30	0.73	IUPHAR
T	Quetiapine	AUG_AP	SINT	150	14.20	14.34	0.97	IUPHAR
U	Escitalopram	SSRI	SINT	10	14.20	14.36	1.14	IUPHAR
V	Vilazodone	SPARI	SINT	20	14.30	14.65	2.45	IUPHAR
W	Mianserin	NaSSA	SINT	30	14.40	14.26	1.00	IUPHAR
X	Sertraline	SSRI	SINT	50	14.50	14.78	1.94	IUPHAR
Y	Paroxetine	SSRI	SINT	20	14.60	14.70	0.68	IUPHAR
Z	Agomelatine	MEL	SINT	25	14.60	14.17	2.95	IUPHAR
AA	Trimipramine	TCA	SINT	50	14.70	14.19	3.45	DrugBank
AB	Valproate	AUG_MS	SINT	500	14.80	14.86	0.38	DrugBank
AC	Citalopram	SSRI	SINT	20	14.80	14.64	1.06	IUPHAR
AD	Levomilnacipran	SNRI	SINT	80	14.90	14.70	1.32	IUPHAR
AE	Moclobemide	MAOI-RIMA	SINT	300	14.90	14.55	2.33	IUPHAR
AF	Milnacipran	SNRI	SINT	50	15.00	14.68	2.15	IUPHAR
AG	Fluoxetine	SSRI	SINT	20	15.10	15.62	3.42	IUPHAR
AH	Amineptine	NDRI	SINT	100	15.20	15.26	0.39	DrugBank
AI	Lamotrigine	AUG_MS	SINT	100	15.20	15.29	0.60	IUPHAR
AJ	Fluvoxamine	SSRI	SINT	100	15.30	15.50	1.28	IUPHAR
AK	Tianeptine	Tianeptine	SINT	12	15.40	15.14	1.66	IUPHAR
AL	Bupropion	NDRI	SINT	150	15.50	15.74	1.53	IUPHAR
AM	Trazodone	SARI	SINT	100	15.80	15.86	0.40	IUPHAR
AN	Hyperforin (Hypericum)	NATURAL	NAT	300	15.80	15.82	0.10	PubChem 451493
AO	Crocin (Saffron)	NATURAL	NAT	30	15.90	16.47	3.58	PubChem 5281232
AP	Zinc	NATURAL	NAT	25	16.70	17.56	5.16	PubChem 23994
AQ	SAMe	NATURAL	NAT	800	16.80	17.10	1.76	PubChem 34706
AR	Cannabidiol (CBD)	NATURAL	NAT	300	16.80	17.44	3.82	PubChem 644019
AS	Vitamin D3	NATURAL	NAT	2000	17.20	16.47	4.22	PubChem 5280795
AT	Curcumin	NATURAL	NAT	1000	17.20	17.81	3.57	PubChem 969516
AU	Magnesium	NATURAL	NAT	400	17.30	17.73	2.46	PubChem 888
AV	Omega-3 EPA	NATURAL	NAT	1000	17.40	16.85	3.17	PubChem 446284
AW	*L. rhamnosus* GG	NATURAL	NAT	10	17.50	16.95	3.13	Tax 47715
AX	Resveratrol	NATURAL	NAT	200	17.50	17.66	0.89	PubChem 445154
AY	Omega-3 DHA	NATURAL	NAT	1000	17.60	16.71	5.07	PubChem 445580

Letter code is stable across all figures and supplementary tables. *Obs./Pred.* in MADRS points at week 8. Placebo summary (18.20, not letter-coded) shown as red dashed line in figures.

Table 2 Per-indicator performance reported for V7. Thresholds were 10% for PK, PD, drug-level, natural-product, and combination rows, and 15% for the remaining rows. The aggregate sample count excludes the placebo summary row.

Indicator	N	MAPE (%)	sMAPE (%)	RMSE	MAE	R^2	Bias	Benchmark
01 PK AUC (3-comp+GFR+2-analyte)	48	0.68	0.66	3.85	2.85	0.999	0.02	FDA DDI
02 PD occupancy (S2+4-target)	48	0.55	0.54	0.53	0.39	0.999	0.01	PET Courtois
03 Kynurenine (IDO1/2+KAT dual)	52	0.36	0.35	0.01	0.007	1.00	0.00	Dantzer
04 GR/FKBP5 (5 CpG+CBG+HPA)	120	0.79	0.78	0.004	0.003	0.971	0.00	Yehuda pyroseq
05 BDNF (sortilin×CaHill×tPA+CREB/HDAC)	110	3.61	3.46	0.11	0.08	0.139	−0.008	Egan/ERK
06 Networks (DTI+GABA E/I+circadian)	100	2.25	2.18	0.02	0.014	0.991	−0.005	Deco DTI
07 MADRS week-8 (anhedonia+MEMS+photo)	300	7.23	7.14	1.19	0.92	0.891	−0.11	Rizvi/Vrijens
07b Placebo	–	2.08	2.10	0.38	0.29	–	−0.21	Kirsch
08 Synthetics per-drug ($N = 39$)	39	1.45	1.40	0.25	0.11	0.926	0.03	Cipriani
09 Naturals per-drug ($N = 12$)	12	3.08	2.95	0.58	0.11	0.260	0.08	RCTs nat.
10 Junctions composite (adj. 15)	15	1.69	1.69	0.27	0.21	0.919	−0.001	Ananth/Su etc.
Mean / maximum	**844**	**2.16 / 7.23**	**2.11**	–	–	–	–	–

The aggregate $N = 844$ is the sum of the non-placebo rows and should not be interpreted as a single jointly measured cohort. Means are calculated from the displayed row-level percentages; RMSE and MAE are not averaged because their units differ across indicators.

Table A1 Extended Data Table 1 – Performance summaries across model versions. MADRS and combination RMSE are shown in separate columns because they summarize different validation targets.

Version	Mean MAPE	Maximum	RMSE_{MADRS}	RMSE_{comb}	R^2_{MADRS}	AUROC	N_{total}
V1 original	12.96%	22.0%	2.89	–	0.032	0.69	329
V2 51 drugs + Bliss	4.94%	12.63%	1.80	–	0.751	0.78	639
V3 circadian	4.38%	12.63%	1.82	–	0.743	0.81	690
V4 residual revision	3.42%	11.49%	1.82	–	0.744	0.84	690
V5 separated indicators	1.94%	7.76%	1.23	–	0.883	0.87	830
V6 ADME/BBB revision	2.22%	7.23%	1.19	–	0.891	0.86	830
V7 composite combinations	**2.16%**	**7.23%**	**1.19**	**0.27**	**0.891**	**0.88**	**844**

The sample counts aggregate separate indicator-level datasets and do not represent one jointly measured cohort.

Table A2 Extended Data Table 2 – Class-level statistics for 51 drugs (V7).

Class	N	Obs MADRS	Pred MADRS	MAPE
SSRI (incl. vortioxetine)	7	14.6 ± 0.48	14.7 ± 0.48	1.41%
SNRI	5	14.34 ± 0.48	14.17 ± 0.20	1.82%
NDRI	2	15.35 ± 0.21	15.49 ± 0.33	0.96%
NaSSA	2	14.05 ± 0.49	13.89 ± 0.51	1.08%
TCA (7)	7	13.68 ± 0.65	13.44 ± 0.55	1.63%
MAOI	3	13.56 ± 1.07	13.32 ± 0.93	1.99%
Atypical/Augment	13	14.25 ± 0.61	14.28 ± 0.53	1.07%
Natural (12)	12	16.97 ± 0.58	17.07 ± 0.42	3.08%
All synthetic (39)	39	14.23 ± 1.08	14.20 ± 0.83	1.45%
Placebo	–	18.20	–	–

Values summarize the 51 drug-level entries provided in the anonymized supplementary data.